Inorg. Chem. **2003**, *42*, 3950–3955

Structures and Magnetic Behavior of 1-, 2-, and 3D Coordination Polymers in the Cu(II)–Dicyanamide–Pyrimidine Family

Jamie L. Manson,*[,†,‡] Jiyeong Gu,[†] John A. Schlueter,[†] and H.-Hau Wang[†]

Materials Science Division, Argonne National Laboratory, 9700 S. Cass Avenue, Argonne, Illinois 60439, and Condensed Matter Sciences Division, Oak Ridge National Laboratory, Oak Ridge, Tennessee 37831

Received November 8, 2002

Using aqueous conditions, three new coordination polymers containing Cu^{2+} cations, dicyanamide (dca) anions, and pyrimidine (pym) were isolated and structurally and magnetically characterized. Comprising the bulk of the product yield, $Cu(dca)_2(pym)_2$, **1**, crystallizes in the monoclinic space group $P2_1/c$ with $a = 7.3569(5)$ Å, $b = 13.4482(9)$ Å, $c = 7.4559(5)$ Å, $\beta = 98.984(3)°$, and $V = 728.6(1)$ Å and forms linear 1D chains. The second compound, $Cu(dca)(NO_3)(pym)(H_2O)$, **2**, is also monoclinic, $P2_1/n$, with $a = 7.6475(3)$ Å, $b = 12.2422(5)$ Å, $c = 11.0286(4)$ Å, $\beta = 106.585(2)°$, and $V = 989.6(1)$ Å^3. A 2D network structure consisting of both bridging μ-dca and pym ligands is formed while the NO_3^- and H_2O are axially bonded to the Cu center. $Cu_3(dca)_6(pym)_2 \cdot 0.75H_2O$, **3**, is triclinic, $P\bar{1}$, with $a = 7.7439(4)$ Å, $b = 9.3388(5)$ Å, $c = 10.1779(5)$ Å, $\alpha = 86.014(2)°$, $\beta = 88.505(2)°$, $\gamma = 73.623(2)°$, and $V = 704.46(9)$ Å^3. The structure of **3** is quite unique in that $[Cu_3(pym)_2]^{6+}$ trimers are interconnected via μ-dca ligands affording a complex 3D self-penetrating framework. Magnetically, **1** exhibits extremely weak exchange interactions along the Cu–$(dca)_2$–Cu ribbons while **2** and **3** display very strong magnetic couplings mediated by the μ-bonded pym ligands. Moreover, **2** shows a broad maximum in $\chi(T)$ at 40 K and behaves as a uniform 1D antiferromagnetic chain with $g = 2.09(1)$, $J/k_B = -42.6(1)$ K, and TIP $= -66 \times 10^{-6}$ emu/mol. An $S = {}^1/_2$ trimer model that includes intertrimer interactions successfully described the magnetic behavior of **3**, yielding $g = 2.10(1)$, $J/k_B = -69.4(5)$ K, $\theta = -0.28(3)$ K, and TIP $= -180 \times 10^{-6}$ emu/mol. It is found that μ-bonded dca and pym ligands mediate very weak and very strong exchange interactions, respectively, between Cu^{2+} centers.

Introduction

Coordination solids composed of paramagnetic cations and organic building blocks such as dicyanamide, $[N(CN)_2]^-$ (herein denoted dca), are the focus of intense research interest, especially among the molecular magnets community.[1] The ability to organize solids into predesigned structures that demonstrate specific physical properties remains very challenging. To this end, we and others have attempted to create various structural motifs by combining divalent first row transition metal ions with dca and auxiliary polyatomic organic ligands.[2,3] Very few of these systems demonstrate long-range magnetic ordering; however, from a structural perspective, many of them are quite fascinating which attests to the coordinative versatility of dca.[1−3] It should be pointed out that a majority of the known metal dca complexes possess low-dimensional (0-, 1-, or 2D) structural motifs while rigid 3D coordination solids occur less often.

* Full address for corresponding author: Center for Neutron Scattering, Condensed Matter Sciences Division, Oak Ridge National Laboratory, Bldg. 7964-I, MS 6430, P.O. Box 2008, Oak Ridge, TN 37831-6430. E-mail: mansonjl@ornl.gov. Phone: +(865) 576-0931. Fax: +(865) 241-1887.

† Argonne National Laboratory.

‡ Oak Ridge National Laboratory.

(1) (a) Manson, J. L.; Kmety, C. R.; Palacio, F.; Epstein, A. J.; Miller, J. S. *Chem. Mater*. **2001**, *13*, 1068. (b) Manson, J. L.; Kmety, C. R.; Epstein, A. J.; Miller, J. S. *Inorg. Chem*. **1999**, *38*, 2552. (c) Kmety, C. R.; Huang, Q.-z.; Lynn, J. W.; Erwin, R. W.; Manson, J. L.; McCall, S.; Crow, J. E.; Stevenson, K. L.; Miller, J. S.; Epstein, A. J. *Phys. Rev. B* **2000**, *62*, 5576. (d) Batten, S. R.; Jensen, P.; Kepert, C. J.; Kurmoo, M.; Moubaraki, B.; Murray, K. S.; Price, D. J. *J. Chem. Soc., Dalton Trans*. **1999**, 2987. (e) Manson, J. L.; Kmety, C. R.; Huang, Q.-z.; Lynn, J. W.; Bendele, G.; Pagola, S.; Stephens, P. W.; Epstein, A. J.; Miller, J. S. *Chem. Mater*. **1998**, *10*, 2552. (f) Batten, S. R.; Jensen, P.; Moubaraki, B.; Murray, K. S.; Robson, R. *Chem. Commun*. **1998**, 439. (g) Kurmoo, M.; Kepert, C. J. *New J. Chem*. **1998**, 1515. (h) Kurmoo, M.; Kepert, C. J. *Mol. Cryst. Liq. Cryst*. **1999**, *334*, 693. (i) Manson, J. L.; Incarvito, C. D.; Rheingold, A. L.; Miller, J. S. *J. Chem. Soc., Dalton Trans*. **1998**, 3705. (j) Manson, J. L.; Incarvito, C. D.; Arif, A. M.; Rheingold, A. L.; Miller, J. S. *Mol. Cryst. Liq. Cryst*. **1999**, *334*, 605.

10.1021/ic026164t CCC: $25.00
Published on Web 05/14/2003

One example of a 3D network solid is ReO_3-like $Mn(dca)_2(pyz)$ {pyz = pyrazine} which has double-interpenetrating lattices.[2] Long-range antiferromagnetic ordering was observed below 2.53(2) K.[2a] At 2 K, field-induced spin flop and paramagnetic phase transitions were observed at 4.3 and 28.3 kOe, respectively, owing to exchange and single ion anisotropies.[2a] Of the $M(dca)_2(pyz)$ series, M = Mn exclusively exhibits 3D magnetic ordering above 2 K.[2,3a]

In our quest for 3D magnetically ordered metal dca compounds, we focused our synthetic efforts on other potentially bridging organic ligands such as pyrimidine (pym). To this end, the divalent first row transition metal ions Mn, Fe, Co, Ni, and Cu were employed. Compounds with M = Fe and Co yield single 3D frameworks and exhibit spin canted ground states below T_N = 3.2 and 1.8 K, respectively, as reported by Ishida and co-workers.[4] In this work, we describe results obtained when Cu is utilized. The aqueous reaction of $Cu(NO_3)_2$, Na(dca), and pym leads to three distinct products, all of which have been obtained as single crystals that can be easily distinguished and mechanically separated. From this single reaction, 1-, 2-, and 3D structures are produced, namely $Cu(dca)_2(pym)_2$, **1**, $Cu(dca)(NO_3)(pym)(H_2O)$, **2**, and $Cu_3(dca)_6(pym)_2{\cdot}0.75H_2O$, **3**. It is worth noting that another phase has been described in which the 3D network, $Cu(dca)_2(pym){\cdot}CH_3CN$, can be obtained from a H_2O/CH_3CN mixture.[5]

Experimental Section

All chemicals were of reagent grade, obtained from commercial sources, and used without further purification.

Synthesis. A 10-mL aqueous solution of $Cu(NO_3)_2{\cdot}2.5H_2O$ (2.15 mmol, 0.500 g) was slowly added with stirring to a 1:1 H_2O/EtOH mixture containing Na(dca) (4.51 mmol, 0.402 g) and pym (4.3 mmol, 0.344 g). A pale blue powder precipitated immediately which was collected via suction filtration and air-dried for 24 h yielding 0.581 g (76%) of **1**. IR $\nu_{C\equiv N}$ (KBr, cm^{-1}): 2414(w), 2310 (s), 2245 (s), and 2178 (vs). Crystals of **1** suitable for a structure determination were obtained by H-tube diffusion of the same reactants over a 1 week period. Elemental analyses and infrared spectroscopy confirmed that the powder and single crystal specimens obtained for **1** are identical. Slow evaporation of the filtrate over a period of 3 days yielded 0.044 g of deep blue single crystals of **2**. IR $\nu_{C\equiv N}$ (KBr, cm^{-1}): 2328 (w), 2277 (w), 2241 (w), 2201 (m), 2189 (m), and 2153 (m). Continued evaporation of the filtrate yielded 0.037 g of yet another compound, namely green crystals of **3**. IR $\nu_{C\equiv N}$ (KBr, cm^{-1}): 2425 (w), 2359 (m), 2324 (m), 2308 (m), 2277 (w), 2258 (m), 2219 (s), and 2176 (s). The three compounds are easily discernible from one another on the basis of color and crystal morphology, thus allowing easy mechanical separation for characterization purposes. Additionally, all three compounds show bands too numerous to list here that are ascribed to pyrimidine stretching and bending modes. Anal. Calcd (%) for $C_{12}H_8N_{10}Cu$, **1**: C, 40.51; H, 2.27; N, 39.37. Found: C, 40.48; H, 2.30; N, 38.94. Anal. Calcd (%) for $C_6H_6N_6O_4Cu$, **2**: C, 24.88; H, 2.09; N, 29.00. Found: C, 24.92; H, 2.19; N, 28.94. Anal. Calcd (%) for $C_{20}H_{9.5}N_{22}O_{0.75}Cu$, **3**: C, 31.65; H, 1.26; N, 40.60. Found: C, 31.43; H, 1.40; N, 39.79.

Table 1. X-ray Crystallographic Data for $Cu(dca)_2(pym)_2$, **1**, $Cu(dca)(NO_3)(pym)(H_2O)$, **2**, and $Cu_3(dca)_6(pym)_2{\cdot}0.75H_2O$, **3**

	1	**2**	**3**
formula	$CuC_{12}N_{10}H_8$	$CuC_6O_4N_6H_6$	$Cu_{1.5}C_{10}O_{0.38}N_{11}H_4$
fw	355.82	289.71	379.55
space group	$P2_1/c$	$P2_1/n$	$P\bar{1}$
a, Å	7.3569(5)	7.6475(3)	7.7439(4)
b, Å	13.4482(9)	12.2422(5)	9.3388(5)
c, Å	7.4559(5)	11.0286(4)	10.1779(5)
α, deg	90	90	86.014(2)
β, deg	98.984(3)	106.585(2)	88.505(2)
γ, deg	90	90	73.623(2)
V, Å^3	728.62(8)	989.57(7)	704.46(6)
Z	2	4	2
ρ_{calcd}, g/cm^3	1.622	1.945	1.789
T, K	295	295	295
λ, Å	0.71073	0.71073	0.71073
μ, mm^{-1}	1.515	2.223	2.304
$R(F)^a$	0.0491	0.0230	0.0285
$R_w(F)^b$	0.1088	0.0625	0.0794
GOF	0.979	1.091	1.047

^{a} $R = \sum[|F_o| - |F_c|]/\sum|F_o|$. ^{b} $R_w = [\sum w[|F_o| - |F_c|]^2/\sum w[|F_o|^2]]^{1/2}$.

X-ray Crystallography. A summary of crystallographic data and selected bond lengths and angles can be found in Tables 1 and 2, respectively. Single crystals of **1**, **2**, and **3** were glued to the end of glass fibers and mounted on a Bruker AXS X-ray diffractometer equipped with a CCD detector. An approximate hemisphere of data was collected for each compound at 295 K using SMART.[6a] The detector frames were integrated by use of the program SAINT[6b] and the intensities corrected for absorption by Gaussian integration using the program SADABS.[6c] Structure solutions were performed using direct methods. Full-matrix least-squares refinements on F^2 (including all data) were carried out using the program SHELXTL.[6d] All non-hydrogen atoms were refined with anisotropic thermal parameters while hydrogen atom positions were located from difference Fourier maps but constrained to ideal geometries using a "riding" model. No correction for extinction was necessary.

Magnetic Measurements. The dc magnetization was measured between 2 and 300 K using a Quantum Design (San Diego, CA) MPMS-7 SQUID magnetometer. Single crystals of each compound were crushed into a fine powder, tightly packed in gelatin capsules, mounted in a plastic straw, and affixed to the end of the sample rod. Samples weighing 40−80 mg were cooled in zero-field to the

(2) (a) Manson, J. L.; Huang, Q.-z.; Lynn, J. W.; Koo, H.-J.; Whangbo, W.-H.; Bateman, R.; Otsuka, T.; Wada, N.; Argyriou, D. N.; Miller, J. S. *J. Am. Chem. Soc*. **2001**, *123*, 162. (b) Manson, J. L.; Incarvito, C. D.; Rheingold, A. L.; Miller, J. S. *J. Chem. Soc., Dalton Trans*. **1998**, 3705. (c) Manson, J. L.; Bordallo, H. N.; Lynn, J. W.; Feyerherm, R.; Loose, A.; Chapon, L. C.; Argyriou, D. N. *Appl. Phys. Lett*., in press. (d) Manson, J. L.; Chapon, L. C.; Bordallo, B. N.; Feyerherm, R.; Argyriou, D. N.; Loose, A. Submitted.

(3) (a) Jensen, P.; Batten, S. R.; Fallon, G. D.; Hockless, D. C. R.; Moubaraki, B.; Murray, K. S.; Robson, R. *J. Solid State Chem*. **1999**, *145*, 387. (b) Vangdal, B.; Carranza, J.; Lloret, F.; Julve, M.; Sletten, J. *J. Chem. Soc., Dalton Trans*. **2002**, 566. (c) Sun, B.-W.; Gao, S.; Ma, B.-Q.; Niu, D.-Z.; Wang, Z. M. *J. Chem. Soc., Dalton Trans*. **2000**, 4187. (d) Escuer, A.; Mautner, F. A.; Sanz, N.; Vicente, R. *Inorg. Chem*. **2000**, *39*, 1668. (e) Sun, B.-W.; Gao, S.; Ma, B.-Q.; Niu, D.-Z.; Wang, Z. M. *New. J. Chem*. **2000**, *24*, 953. (f) Sun, B.-W.; Gao, S.; Ma, B.-Q.; Niu, D.-Z.; Wang, Z. M. *Inorg. Chem. Commun*. **2001**, *4*, 72. (g) van Albada, G. A.; Quiroz-Castro, M. E.; Mutikainen, I.; Turpeinen, U.; Reedijk, J. *Inorg. Chim. Acta*, **2000**, *298*, 221. (h) Hvastijová, M.; Kozís×c1ek, J.; Kohout, J.; Jäger, L.; Fuess, H. *Transition Met. Chem*. **1995**, *20*, 276.

(4) Kusaka, T.; Ishida, T.; Hashizume, D.; Iwasaki, F.; Nogami, T. *Chem. Lett*. **2000**, 1146.

(5) Riggio, I.; van Albada, G. A.; Ellis, D. D.; Spek, A. L.; Reedijk, J. *Inorg. Chim. Acta*. **2001**, *313*, 120.

(6) (a) *SMART, Version 5.054, Data Collection Software*; Bruker AXS, Inc.: Madison, WI, 1999. (b) *SAINT, Version 5.00, Data Integration Software*; Bruker AXS, Inc.: Madison, WI, 1999. (c) Sheldrick, G. M. *SADABS, Version 2.01*; University of Göttingen: Göttingen, Germany, 1996. (d) *SHELXTL, Version 5.0, Structure Solution and Refinement Software*; Bruker AXS, Inc.: Madison, WI, 1996.

Table 2. Selected Interatomic Distances (Å) and Angles (deg) for $Cu(dca)_2(pym)_2$, **1**, $Cu(dca)(NO_3)(pym)(H_2O)$, **2**, and $Cu_3(dca)_6(pym)_2 \cdot 0.75H_2O$, **3**

		$Cu(dca)_2(pym)_2$, **1**			
Cu−N(1)	1.995(4)	N(1)−Cu−N(1′)	180.0	N(4)−Cu−N(4′)	180.0
Cu−N(3)	2.425(4)	N(1)−Cu−N(3)	89.8(1)	C(1)−N(1)−Cu	168.3(3)
Cu−N(4)	2.033(3)	N(1)−Cu−N(4)	89.6(1)	C(2)−N(3)−Cu	140.5(4)
C(1)−N(1)	1.139(5)	N(3)−Cu−N(4)	89.9(1)	N(1)−C(1)−N(2)	172.8(4)
		$Cu(dca)(NO_3)(pym)(H_2O)$, **2**			
Cu−N(1)	1.993(1)	N(1)−Cu−N(3)	179.03(6)	N(5)−Cu−O(1)	86.03(5)
Cu−N(3)	1.979(1)	N(1)−Cu−N(5)	92.35(6)	N(5)−Cu−O(4)	91.08(5)
Cu−N(5)	2.024(1)	N(1)−Cu−N(6)	91.57(5)	N(6)−Cu−O(1)	91.30(5)
Cu−N(6)	2.038(1)	N(1)−Cu−O(4)	87.36(6)	N(6)−Cu−O(4)	92.11(5)
Cu−O(1)	2.498(1)	N(1)−Cu−O(1)	85.13(5)	O(1)−Cu−O(4)	171.84(5)
Cu−O(4)	2.319(1)	N(3)−Cu−N(5)	87.61(6)	C(1)−N(1)−Cu	162.8(1)
C(1)−N(1)	1.145(2)	N(3)−Cu−N(6)	88.42(6)	C(2)−N(3)−Cu	164.1(2)
C(1)−N(2)	1.307(2)	N(3)−Cu−O(1)	93.90(6)	N(1)−C(1)−N(2)	174.1(2)
C(2)−N(2)	1.301(2)	N(3)−Cu−O(4)	93.60(6)	N(2)−C(2)−N(3)	171.7(2)
C(2)−N(3)	1.145(2)	N(5)−Cu−N(6)	175.06(5)	C(1)−N(2)−C(2)	120.4(2)
		$Cu_3(dca)_6(pym)_2 \cdot 0.75H_2O$, **3**			
Cu(1)−N(1)	1.970(2)	N(1)−Cu(1)−N(1′)	180.0	N(5)−Cu(2)−N(11)	176.69(8)
Cu(1)−N(4)	2.449(2)	N(1)−Cu(1)−N(10)	90.05(7)	N(7)−Cu(2)−N(8)	107.23(8)
Cu(1)−N(10)	2.049(2)	N(4)−Cu(1)−N(4′)	180.0	N(7)−Cu(2)−N(11)	88.59(8)
Cu(2)−N(3)	1.987(2)	N(10)−Cu(1)−N(10′)	180.0	C(1)−N(1)−Cu(1)	171.7(2)
Cu(2)−N(5)	1.966(2)	N(1)−Cu(1)−N(4)	86.54(9)	C(3)−N(4)−Cu(1)	147.2(2)
Cu(2)−N(7)	2.198(2)	N(4)−Cu(1)−N(10)	90.29(7)	C(2)−N(3)−Cu(2)	174.4(2)
Cu(2)−N(8)	1.987(2)	N(3)−Cu(2)−N(5)	91.46(9)	C(4)−N(5)−Cu(2)	168.4(2)
Cu(2)−N(11)	2.081(2)	N(3)−Cu(2)−N(7)	98.69(9)	C(5)−N(7)−Cu(2)	158.7(2)
		N(3)−Cu(2)−N(8)	154.08(9)	C(6)−N(8)−Cu(2)	153.7(2)
		N(3)−Cu(2)−N(11)	90.16(8)	N(1)−C(1)−N(2)	171.4(2)
		N(5)−Cu(2)−N(7)	94.01(9)	N(4)−C(3)−N(6)	172.3(3)

lowest temperature of 2 K. The dc field was then charged to 1 kOe, and data were recorded upon warming. All magnetic data were corrected for core diamagnetism using Pascal's constants.

Results and Discussion

Crystal Structures. $Cu(dca)_2(pym)_2$, 1. Each Jahn−Teller distorted Cu ion is coordinated to four different dca ligands in the equatorial plane and two monodentate pym ligands as shown in Figure 1. The CuN_6 chromophore consists of two Cu−N(1), Cu−N(3), and Cu−N(4) bond distances of 1.995(4), 2.425(4), and 2.033(3) Å, respectively. The *cis*-N−Cu−N′ bond angles deviate slightly from O_h symmetry and range from 89.6(1)° to 90.4(1)°. As expected, the dca anions do not coordinate linearly to the metal center, exhibiting C(1)−N(1)−Cu and C(2)−N(3)−Cu angles of 168.3(3)° and 140.5(4)°, respectively. The bond distances and angles within the dca and pym moieties are typical of these species.

The extended structure of **1** is a linear 1D chain (Figure 2) similar to $Mn(dca)_2(py)_2$.[7] Each dca is μ-bonded to two different Cu cations. Edge-sharing CuN_6 octahedra are connected via four different dca anions giving intrachain Cu···Cu distances of 7.456 Å. The chains are interdigitated and pack along the *b*-axis in an undulating fashion so as to form weakly held quasi-2D layers (ring $\pi-\pi$ distances ~3.7 Å) as shown in Figure 3. This undulating arrangement is similar to that found in $Mn(dca)_2(pym)_2$ but contrasts with that of $Mn(dca)_2(py)_2$ which packs in a planar fashion.[7,8] This suggests that although the pym ligands in **1** are nonbridging, the weak $\pi-\pi$ interactions between stacked pym ligands may influence the observed packing scheme. The interchain Cu···Cu separations within a quasi-2D layer are 7.688 Å.

$Cu(dca)(NO_3)(pym)(H_2O)$, 2. The structure of **2** consists of tetragonally distorted Cu^{2+} centers that are bonded by four nitrogen atoms from two dca and two pym ligands (Figure 4). The axial positions are occupied by coordinated H_2O and NO_3^- molecules that protrude above and below the plane. As the metal ion does not occupy a special position, the four Cu−N and two Cu−O bond distances are inequivalent

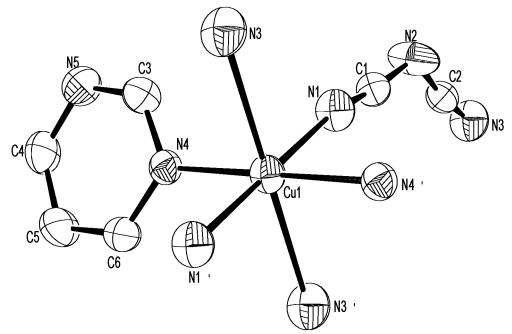

Figure 1. ORTEP and atom labeling diagram for $Cu(dca)_2(pym)_2$, **1**. Thermal ellipsoids are drawn at the 30% level. Hydrogen atoms have been omitted for clarity.

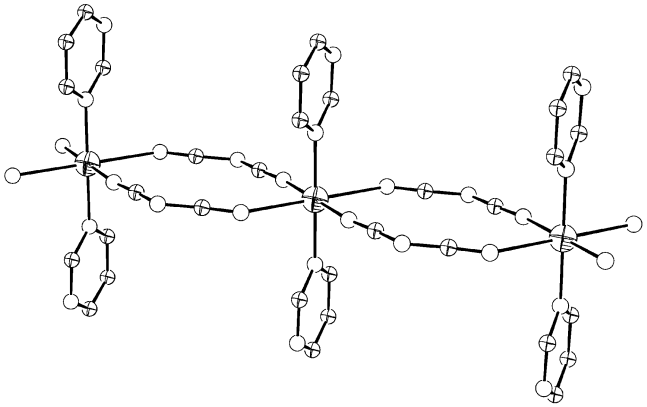

Figure 2. Segment of a single 1D linear chain observed in $Cu(dca)_2(pym)_2$, **1**. Hydrogen atoms have been omitted for clarity.

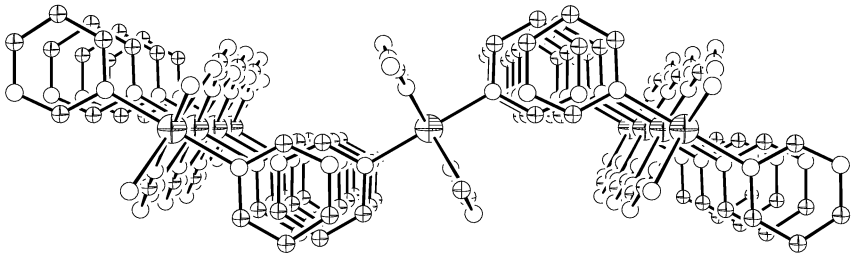

Figure 3. Illustration viewed down the *c*-axis depicting the undulated chain packing found in $Cu(dca)_2(pym)_2$, **1**. Hydrogen atoms have been omitted for clarity.

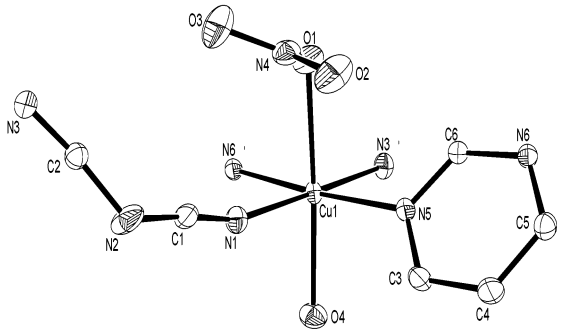

Figure 4. ORTEP and atom labeling diagram for $Cu(dca)(NO_3)(pym)(H_2O)$, **2**. Thermal ellipsoids are drawn at the 30% level. Hydrogen atoms have been omitted for clarity.

[Cu−N(1) = 1.993(1) Å, Cu−N(3) = 1.980(1) Å, Cu−N(5) = 2.025(1) Å, Cu−N(6) = 2.039(1) Å, Cu−O(1) = 2.498(1) Å, and Cu−O(4) = 2.318(1) Å]. The CuN_4O_2 chromophore is somewhat squashed with O(4)−Cu−N(1) and O(4)−Cu−N(3) bond angles of 87.40(6)° and 93.57(6)°, respectively. Similar to **1** and **3**, the dca anions adopt nonlinear bonding configurations about the Cu ion with C(1)−N(1)−Cu = 162.8(1)° and C(2)−N(3)−Cu = 164.2(1)°.

Linear chains of Cu−dca−Cu single ribbons are cross-linked by Cu−pym−Cu chains so as to form a 2D layered structure as shown in Figure 5. Hydrogen bond interactions between the H_2O and amide N-atom [O(4)−H(4B)···N(2) = 3.116 Å] hold the layers together and stabilize the 3D framework. Intralayer Cu···Cu separations are, respectively, 7.559 and 5.750 Å and coincide with Cu−dca−Cu and Cu−pym−Cu interactions while the closest intermolecular Cu···Cu distance is 6.881 Å. Moreover, neighboring octahedra are considerably tilted with respect to one another.

$Cu_3(dca)_6(pym)_2\cdot 0.75H_2O$, 3. Trimeric units consisting of two types of Cu^{2+} coordination geometries were observed (Figure 6). Located at the center of inversion, Cu(1) is tetragonally elongated while Cu(2) is a distorted square pyramid and occupies a general position. The metal coordination spheres of both Cu ions consist entirely of nitrogen atoms from pym and dca ligands. The equatorial positions of Cu(1) are composed of two coordinated dca [Cu(1)−N(1) = 1.970(2) Å] and two pym ligands [Cu(1)−N(10) = 2.049(2) Å] while the axial positions are longer and occupied by the other two dca anions [Cu(1)−N(4) = 2.449(2) Å].

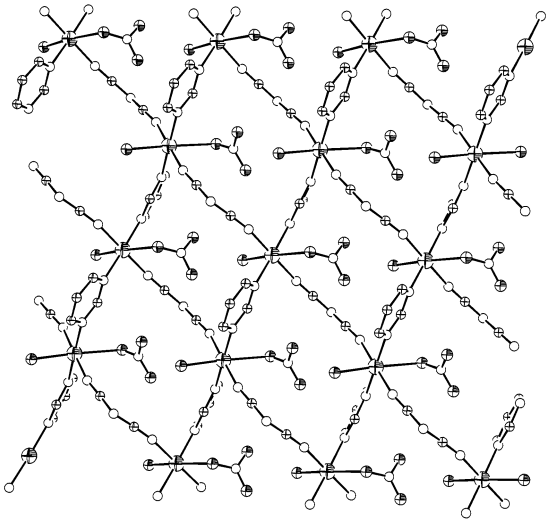

Figure 5. Extended 2D gridlike layer found in $Cu(dca)(NO_3)(pym)(H_2O)$, **2**. Hydrogen atoms have been omitted for clarity.

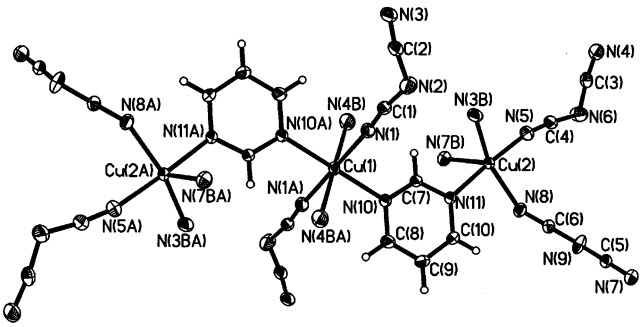

Figure 6. ORTEP and atom labeling diagram of the "trimeric" unit found in $Cu_3(dca)_6(pym)_2\cdot 0.75H_2O$, **3**. Thermal ellipsoids are drawn at the 30% level.

The CuN_6 chromophore is somewhat distorted, with N(1)−Cu(1)−N(4) and N(4)−Cu(1)−N(10) bond angles of 86.54(9)° and 90.29(7)°, respectively. Cu(1) is connected to Cu(2) via an intervening pym ligand at a distance of 5.790 Å. The Cu(2) coordination geometry consists of three basal μ-dca's [Cu(2)−N(3) = 1.988(2) Å, Cu(2)−N(7) = 2.199(2) Å, and Cu(2)−N(8) = 1.977(2) Å] and one apical μ-dca [Cu(2)−N(5) = 1.966(2) Å] while the fourth basal site is occupied by the pym ligand which has a Cu(2)−N(11) distance of 2.081(2) Å. Cu(2) is connected to Cu(2A) by three different dca ligands. These Cu−N distances compare favorably to those observed in other systems such as $Cu(dca)_2$ and $Cu(dca)_2(apym)_2$ {apym = 2-aminopyrimidine}.[1f,3g] The distortion of the square pyramid is readily apparent from the N(3)−Cu(2)−N(8), N(3)−Cu(2)−N(7), and N(7)−

(7) Manson, J. L.; Arif, A. M.; Incarvito, C. D.; Liable-Sands, L. M.; Rheingold, A. L.; Miller, J. S. *J. Solid State Chem.* **1999**, *145*, 369.
(8) Manson, J. L.; Schlueter, J. A. Manuscript in preparation.

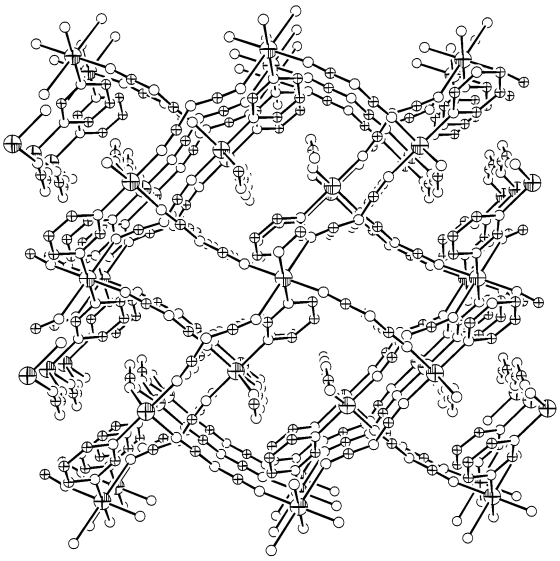

Figure 7. Self-penetrated 3D network structure of $Cu_3(dca)_6(pym)_2 \cdot 0.75H_2O$, **3**. The disordered water molecule and all hydrogen atoms have been omitted for clarity.

Cu(2)−N(8) bond angles which are 154.08(9)°, 98.69(9)°, and 107.23(8)°, respectively. As generally observed, the nitrile substituent of the dca ligands does not coordinate linearly to the metal center, giving respective Cu(1)−N(1)−C(1), Cu(1)−N(4)−C(3), Cu(2)−N(3)−C(2), Cu(2)−N(5)−C(4), Cu(2)−N(7)−C(5), and Cu(2)−N(8)−C(6) bond angles of 171.7(2)°, 147.2(2)°, 174.4(2)°, 168.4(2)°, 158.7(2)°, and 153.7(2)°. The bond distances and angles of dca and pym are typical of these ligands.

The trinuclear units are interconnected to one another by dca ligands in multiple directions to afford an unusual self-penetrating 3D polymeric array, Figure 7.[9] Cu(1) is further connected to Cu(2) by four dca bridges at distances of 7.995 and 8.509 Å while three different dca ligands couple Cu(2) to Cu(2a) at distances of 7.744 Å. Within the network resides a partially occupied (and disordered) H_2O molecule that is located ~3.23 Å from the nearest amide nitrogen N(6) of a dca ligand. As far as we are aware, this is the first example of a self-penetrating 3D structure comprised of clusterlike building blocks.

Magnetic Behavior. $Cu(dca)_2(pym)_2$, 1. The temperature-dependent magnetic behavior of **1** indicates the presence of very weak exchange interactions as typical of alternating axial/equatorial Cu−dca−Cu bridges. At room temperature, $\chi T(T)$ has a value of 0.40 emu K/mol that is consistent with the value expected for $S = {}^1/_2$ Cu^{2+} ions. Upon cooling to low temperature, $\chi T(T)$ does not vary greatly as anticipated for a Curie-like system until ~5 K where a small downturn is noted. A fit of the data to the Bonner−Fisher[10] antiferromagnetic chain model yields $g = 2.083(1)$ and very small $J/k_B = -0.033(5)$ K. Such small values of J/k_B have been observed in other Cu−dca compounds including $Cu(dca)_2$ itself.[1f] The $1/\chi$ data can be fitted to a Curie−Weiss law with $g = 2.074(1)$ and $\theta = -0.61(3)$ K which indicates extremely weak antiferromagnetic coupling between Cu^{2+} ions. Expectedly, no 3D magnetic ordering was observed above 2 K.

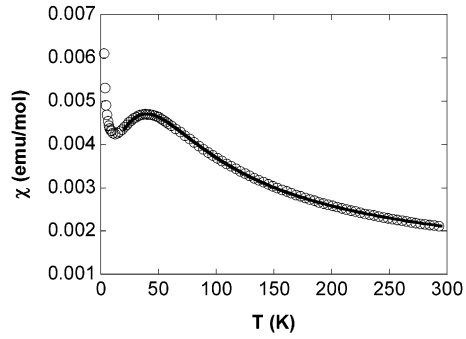

Figure 8. Temperature variation of $\chi(T)$ for $Cu(dca)(NO_3)(pym)(H_2O)$, **2**. Because the exchange interaction is largely negligible along the Cu−dca−Cu chain and much stronger along the Cu−pym−Cu component, the data were fitted to a uniform AFM chain model as described in the text.

$Cu(dca)(NO_3)(pym)(H_2O)$, 2. Figure 8 displays the magnetic susceptibility data for **2** taken between 2 and 300 K. A broad maximum in $\chi(T)$ is observed at 40 K that suggests low-dimensional magnetic exchange between Cu^{2+} ions. Below about 12 K the susceptibility rises abruptly. This increase is often ascribed to defects in the crystal lattice or the presence of paramagnetic impurities although it has recently been pointed out that it could also be due to staggered (or alternately aligned) *g*-tensors. Such behavior has been addressed in detail for the $Cu(PhCO_2)_2 \cdot 3H_2O$[11] and $Cu(NO_3)_2(pym)(H_2O)_2$[12] linear chain compounds. By virtue of the structure of **2**, the counter-rotated CuN_4O_2 octahedra can certainly manifest a similar effect. A Curie−Weiss fit of $1/\chi$ between 70 and 300 K yields $g = 2.10(1)$ and $\theta = -124.03(2)$ K which is indicative of strong antiferromagnetic interactions between Cu sites. Since the Jahn−Teller distortion lies along the O−Cu−O′ axis, this infers that the Cu ions are all connected to one another by equatorial pym and dca bridge interactions. With regard to Cu−dca−Cu coupling, it has been demonstrated in rutile-like $Cu(dca)_2$ that equatorial dca bridges still lead to rather weak magnetic interactions.[1f,g] As the Cu ions along the Cu−pym−Cu chains are equidistant and very weak coupling is known to occur along Cu-dca-Cu pathways, $\chi(T)$ was fitted between 20 and 300 K to the Bonner−Fisher expression[13] for a uniform S $= {}^1/_2$ chain giving $g = 2.09(1)$ and $J/k_B = -42.6(1)$ K. By comparison, for $Cu(dca)_2(pym) \cdot CH_3CN$ and $Cu(NO_3)_2(pym)(H_2O)_2$ which also feature μ-pym components, very weak

(9) The term self-penetrating network is used here because it refers to a single network that entangles itself. This contrasts with interpenetrating as it refers to multiple networks that entangle one another. Recent examples of self-penetrating networks include the following: (a) Jensen, P.; Price, D. J.; Batten, S. R.; Moubaraki, B.; Murray, K. S. *Chem. Eur. J.* **2000**, *6*, 3186. (b) Carlucci, L.; Ciani, G.; Proserpio, D. M.; Rizzato, S. *J. Chem. Soc., Dalton Trans.* **2000**, 3821. (c) Abrahams, B. F.; Batten, S. R.; Grannas, M. J.; Hamit, H.; Hoskins, B. F.; Robson, R. *Angew. Chem., Int. Ed.* **2000**, *39*, 1506.

(10) Bonner, J. C.; Fisher, M. E. *Phys. Rev. A* **1964**, *135*, 640.

(11) (a) Dender, D. C.; Hammar, P. R.; Reich, D. H.; Broholm, C.; Aeppli, G. *Phys. Rev. Lett.* **1997**, *79*, 1750. (b) Dender, D. C.; Davidovic, D.; Reich, D. H.; Broholm, C.; Lefmann, K.; Aeppli, G. *Phys. Rev. B* **1996**, *53*, 2583.

(12) (a) Yasui, M.; Ishikawa, Y.; Akiyama, N.; Ishida, T.; Nogami, T.; Iwasaki, F. *Acta Crystallogr.* **2001**, *B57*, 288. (b) Feyerherm, R.; Abens, S.; Günther, D.; Ishida, T.; Meissner, M.; Meschke, M.; Nogami, T.; Steiner, M. *J. Phys.: Condens. Matter* **2000**, *12*, 8495.

(13) Bonner, J. C.; Fisher, M. E. *Phys. Rev. B* **1964**, *135*, A640.

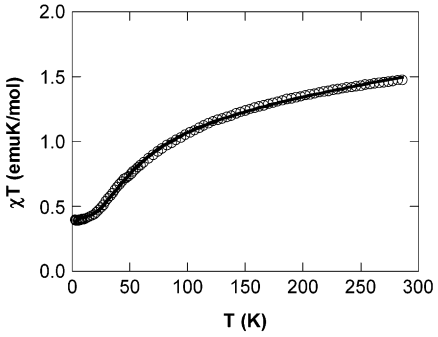

Figure 9. Temperature dependence of χT for $Cu_3(dca)_6(pym)_2 \cdot 0.75H_2O$, **3**. The solid line denotes the least-squares fit of the data to the theoretical expression described in the text.

and moderate magnetic interactions of >-1 K and -18 K were observed, respectively.[5,12] Attempts to fit $\chi(T)$ for **2** over a broader temperature range by considering possible paramagnetic impurities lead to extremely poor agreement. This result further substantiates our claim for staggered field effects. Collectively, these effects render it difficult to assess possible interlayer exchange interactions.

$Cu_3(dca)_6(pym)_2 \cdot 0.75H_2O$, 3. The temperature-dependent magnetic susceptibility of **3** has been measured between 2 and 300 K and is shown in Figure 9 in the form of $\chi T(T)$. $\chi T(T)$ decreases continuously upon cooling from room temperature down to ~25 K owing to strong antiferromagnetic interactions between the Cu^{2+} spins. Below 25 K, χT reaches a plateau with a nominal value of 0.40 emu K/mol that is consistent with residual paramagnetism associated with an odd number of Cu^{2+} sites. This behavior is similar to that observed in a variety of largely isolated trimeric assemblies.[14] Since the crystal structure of **3** does indeed consist of trinuclear entities, the strong exchange coupling exhibited must arise from the Cu^{2+} spin−spin interaction propagated by the pym bridging ligands. The magnetic data are well reproduced by the expression for an $S = {}^1/_2$ linear trimer $\{H = -J[S_1 \cdot S_2 + S_2 \cdot S_3] - J'[S_1 \cdot S_3]\}$ modified to include intertrimer interactions (eq 1) giving $\langle g \rangle = 2.10(1)$, $J/k_B = -69.4(5)$ K, $\theta = -0.28(3)$ K, and TIP $= 180 \times 10^{-6}$ emu/mol.[14a,15] The obtained g-value is the average of the three Cu^{2+} ions, and the large temperature-independent paramagnetism, TIP, represents the entire trinuclear species, which is 60×10^{-6} emu/mol per Cu^{2+} ion. The small θ-value denotes a feeble antiferromagnetic exchange interaction between trimeric units mediated by the Cu(1)−dca−Cu(2) and Cu(2)−dca−Cu(2A) bridges. The strong superexchange coupling energy observed for the Cu(1)−pym−Cu(2) bridge is the largest value observed thus far.[16] We reason that a $d_{xy}/d_{x^2-y^2}$ magnetic ground state for Cu(2) leads to an increased number of antiferromagnetic interactions and thus a larger J-value. No long-range magnetic ordering was observed owing to the weak intertrimer interactions.

$$\chi_M = \frac{N\beta^2 g^2}{3k(T-\theta)}\left(\frac{1.5 + 1.5e^{J/kT} + 15e^{3J/2kT}}{2 + 2e^{J/kT} + 4e^{3J/2kT}}\right) + \text{TIP} \quad (1)$$

Conclusion

We have further demonstrated the utility of the dca anion in assembling novel structural and magnetic systems, especially when combined with bridging organic ligands such as pyrimidine. Although only weak exchange interactions are mediated by μ-bridged dca anions, its continued use in the design of molecular magnetic materials may lead to other novel structures, and presumably more of them will demonstrate long-sought bulk magnetic ordering phenomena or new magnetic ground states.

Acknowledgment. Work at Argonne National Laboratory is supported by the Office of Basic Energy Sciences, Division of Materials Science, U.S. Department of Energy under Contract W-31-109-ENG-38. Oak Ridge National Laboratory is managed by UT-Battelle, LLC for the U.S. Department of Energy under Contract DE-AC05-00OR22725.

Supporting Information Available: Crystallographic data in CIF format. This material is available free of charge via the Internet at http://pubs.acs.org.

IC026164T

(14) See for example: (a) Zhao, L.; Thompson, L. K.; Xu, Z.; Miller, D. O.; Stirling, D. R. *J. Chem. Soc., Dalton Trans*. **2001**, 1706. (b) Gao, E.-Q.; Zhao, Q.-H.; Tang, J.-K.; Liao, D.-Z.; Jiang, Z.-H.; Yan, S.-P. *J. Chem. Soc., Dalton Trans*. **2001**, 1537. (c) Journaux, Y.; Sletten, J.; Kahn, O. *Inorg. Chem*. **1986**, *25*, 439. (d) Garcia, A.; Costa, R.; Ribas, J. *Inorg. Chem. Acta*. **1990**, *168*, 249. (e) Veit, R.; Girerd, J.-J.; Kahn, O.; Robert, F.; Jeannin, Y. *Inorg. Chem*. **1986**, *25*, 4175.

(15) Kahn, O. *Molecular Magnetism*; VCH: New York, 1993.

(16) (a) Nakayama, K.; Ishida, T.; Takayama, R.; Hashizume, D.; Yasui, M.; Iwasaki, F.; Nogami, T. *Chem. Lett*. **1998**, 497. (b) Ishida, T.; Nakayama, K.; Nakagawa, M.; Sato, W.; Ishikawa, Y.; Yasui, M.; Iwasaki, F.; Nogami, T. *Synth. Met*. **1997**, *85*, 1655. (c) Nakayama, K.; Nakagawa, M.; Ishida, T.; Ishikawa, Y.; Yasui, M.; Iwasaki, F.; Nogami, T. *Mol. Cryst. Liq. Cryst*. **1997**, *306*, 379. (d) Nakagawa, M.; Ishikawa, Y.; Kogane, T.; Ishida, T.; Yasui, M.; Iwasaki, F.; Nogami, T. *Mol. Cryst. Liq. Cryst*. **1996**, *286*, 29. (e) Ishida, T.; Nogami, T.; Yasui, M.; Iwasaki, F.; Iwamura, H.; Takeda, N.; Ishikawa, M. *Mol. Cryst. Liq. Cryst*. **1996**, *279*, 87. (f) Ishida, T.; Mitsubori, S.-I.; Nogami, T.; Ishikawa, Y.; Yasui, M.; Iwasaki, F.; Iwamura, H.; Takeda, N.; Ishikawa, M. *Synth. Met*. **1995**, *71*, 1791. (g) Ishida, T.; Mitsubori, S.-I.; Nogami, T.; Iwamura, H. *Mol. Cryst. Liq. Cryst*. **1993**, *233*, 345. (h) Mitsubori, S.-I.; Ishida, T.; Nogami, T.; Iwamura, H. *Chem. L ett*. **1994**, 285. (i) Lloret, F.; De Munno, G.; Julve, M.; Cano, J.; Ruiz, R.; Canneschi, A. *Angew. Chem., Int. Ed*. **1998**, *37*, 135.